Mapping Small-Scale Mining Sites in Wassa Amenfi East Area of Ghana*

[1]F. F. Howard, [1]C. B. Boye, [1]I. Yakubu, and [1]J. S. Y. Kuma
[1]University of Mines and Technology, Tarkwa, Ghana

Howard, F. F., Boye, C. B., Yakubu, I., and Kuma, J. S. Y. (2023) "Mapping Small-Scale Mining Site in Wassa Amenfi East Area of Ghana", *Ghana Journal of Technology*, Vol. 7, No. 2, pp. 1 - 9.

Abstract

Environmental degradation brought on by legal and illegal small-scale mining activities has become a major issue in Ghana. The ecosystems and communities that are close to mining sites are seriously threatened. Unmanned Aerial Vehicles (UAVs) with cameras are used to gather photographs of small-scale mining areas as part of a solution that is put out to help monitor and solve this issue. A UAV fitted with photogrammetry sensors for mapping an inaccessible mining location in the Wassa Amenfi East area of Ghana was adopted for the data collection. DJI Phantom 4 Pro v2 drone was used to collect high-resolution images; Global Navigation Satellite System (GNSS) receivers were used to establish Ground Control Points (GCP); and SimActive Correlator 3D software was employed in the processing of images of the area. Based on the GCPs, accuracy assessment and statistical analysis were carried out. An average Root Mean Square Error (RMSE) of 0.008 m and 0.034 m were obtained for the horizontal and vertical positions, respectively. The findings demonstrate that the combination of unmanned aerial vehicles and photogrammetry offers a risk-free, more effective, and reasonably priced method for mapping inaccessible abandoned or active mine sites, enabling the generation of accurate surface models for landform reclamation and management.

Keywords: Unmanned Aerial Vehicles, Real-Time Kinematic GNSS, Landform Reclamation, Mine Sites

1 Introduction

Small-scale gold mining has gained significance in West Africa due to its contribution to the creation of wealth and employment opportunities for its citizens, as well as its usefulness to the country's economy. However, the activities of these small-scale gold miners expose the land and surface water bodies to toxic mercury, which pollutes the soil and surface water bodies. Also, the faces of the landscapes and their scenery are greatly degraded. This has resulted in poor agricultural yield, thus jeopardising food security and access to safe drinking water. Government efforts to control the activities of these miners have often proved futile, as most of the nefarious activities are carried out in obscured locations that are often not easily accessible by road. The application of conventional ways of surveying in such an environment is cumbersome, risky, time-consuming, and expensive; thus, topographic surveys of the same quality as those of the traditional methods are required, but in a fraction of the time (Kellenberger *et al.*, 2018).

The use of UAV to map inaccessible small-scale mining sites is examined in this paper using the DJI Phantom 4 Pro V2. The study site is part of the Wassa Amenfi East District, which is located in difficult terrain, is degraded, and has proved challenging to reach. However, the DJI Phantom 4 Pro V2's advanced capabilities offer a creative approach to mapping such a place.

UAVs (drones) can safely and efficiently go to difficult-to-reach small-scale gold mining sites, minimising surveyors' danger. Both Culig *et al*. (2018) and Daz-Vilario *et al*. (2019) have highlighted how drones may safely cross difficult terrain, enter hazardous sites, and acquire data without endangering personnel. By taking high-resolution images of abandoned, inaccessible small-scale gold mining sites, the UAV (i.e., the DJI Phantom 4 Pro V2), known for its remarkable aerial photography capabilities, surpasses conventional mapping methods. It offers precise and reliable data collection because of its one-inch CMOS sensor, mechanical shutter, and 20-megapixel camera. Researchers like Khodabandeloo *et al*. (2019), Hu *et al*. (2020), and Hao *et al*. (2019) have noted that the UAV's capacity to swiftly gather high-resolution data utilising LiDAR and photogrammetry sensors can be useful for small-scale gold mining sites with limited time and resources.

Additionally, drone mapping using ground control points (GCPs) is more affordable than traditional surveying techniques. Elfadaly *et al.* (2017), Amiri *et al*. (2019), Ghosh *et al*. (2018), and Singh *et al*. (2020) have highlighted the reduced need for expensive equipment and extensive labour, resulting in lower operational costs. Studies by Smith *et al*. (2022) have shown the potential of UAVs, particularly the DJI Phantom 4 Pro V2, in precisely assessing closed mines, spotting potential dangers, and aiding restoration initiatives in the Appalachian region.

**Manuscript received June 14, 2023*
Revised version accepted September 19, 2023

The development of accurate orthomosaic maps and three-dimensional models of difficult terrain is made possible by the combination of photogrammetry methods with UAV imagery using software like SimActive Corelator 3D. Johnson and Brown (2021) have produced accurate and scalable reconstructions of abandoned mining sites by fusing UAV technology with photogrammetry.

Overall, the use UAVs, allows for effective exploration of difficult-to-reach small-scale mining locations. Environmental hazards can be recognised by mapping and data collection, allowing for more informed decisions for the preservation of these areas.

The difficulties of mapping an abandoned mine site using conventional surveying techniques were studied by Koltunov *et al*. (2019). It was discovered that conventional surveying methods were inappropriate for this kind of project due to the challenging terrain, which made it impossible to collect accurate data. In a study by Beyer *et al*. (2017), the use of UAVs for surveying inaccessible mine sites was investigated. UAVs and photogrammetry could be used to collect very accurate survey data while posing less danger to survey teams. It was concluded that UAV technologies provide an easier, safer, and more affordable method of mapping inaccessible mining regions. Therefore, this paper sought to determine the locations of small-scale gold mining sites in real-time using UAVs and RTK GNSS techniques to ensure effective monitoring of their operations in order to preserve the environment.

2 Materials and Method Used

2.1 The Study Area

According to Figure 1, the Wassa Amenfi East District is situated in the center of the western region of Ghana. It is positioned between Latitudes 5° N and 6° N and Longitudes 1° W and 2° W. With a total geographical area of 1600 km^2, the Wassa Amenfi East District makes up roughly 7.5% of the Western Region's overall area. By road, Sekondi-Takoradi, the regional capital, is 180 kilometers away. The inhabitants of the district depend largely on Kumasi, located in the Ashanti region, for their economic activities.

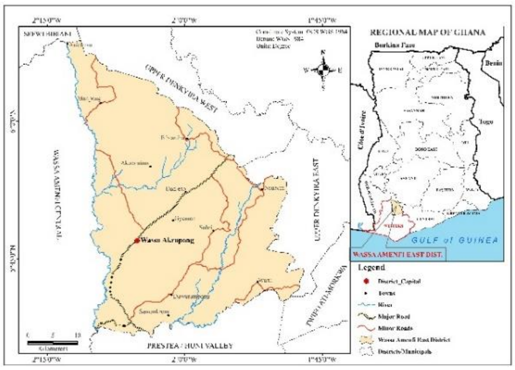

Fig. 1 Map of Wassa Amenfi East Districts

2.2 Materials

DJI Phantom 4 Pro v2, Real Time Kinematic (RTK) GNSS receivers, and SimActive Correlator 3D software were used for the acquisition and processing of the data.

The DJI Phantom 4 Pro has rotary wings. For shooting in amateur broadcasting, this is frequently utilised. It is a tiny UAV that weighs only 1.24 kg and can fly at a top speed of 15 m/s. A 20-megapixel (MP) camera is also included, and it offers a real-time link between the camera and a smartphone. Despite being a product for entertainment, the Phantom 4 Pro has been effectively utilized for surveying work, despite the fact that it is challenging to attach additional devices to the body.

The Remote Controller of the Phantom 4 Pro has a Maximum Transmission Distance of 7 km (unobstructed and free of interference). The Camera sensor is 1" CMOS, the effective pixels: 20 M, and the lens has a FOV of 84°, 8.8 mm/24 mm (35 mm format equivalent). f/2.8–f/11 autofocus at 1m∞, ISO Range: 100–3200 (Auto), 100–6400 (Manual), Mechanical Shutter Speed: 8–1/2000 s; Electronic Shutter Speed: 8–1/2000 s. (DJI, 2017).

S9111 Plus Dual Frequency Channels: 220; Satellite Tracked: GPS; GLONASS: (GLONASS M Only); GNSS 220ch GPRS with UHF 410/470 MHz was used for the RTK survey of all the GCPs.

2.3 Method Used

Fig. 2 shows the work flowchart of the methods used.

2.3.1 Building of Ground Control Points

GCPs provide the means for orientation or relating aerial photographs to the ground. GCPs are generally classified as either horizontal control or vertical control. The World Geodetic System (WGS) 1984 and the Local Spheroid Clarke 1880 (UTM/WGS 84/UTM zone 30 N) coordinate projection systems were used in establishing the GCPs. The generated images of the GCPs must be clear, well-defined, positively identified on all photos, and located in advantageous locations in the photographs (Madawalagama et al., 2016; Korpela, 2004). GCPs are utilized for more accurate results since they are measured using a more precise technique of measuring position. For validation of the survey work, six temporal controls were established within the boundary of the study area. This was done to distribute the pillars throughout the entire study area to minimize distortions. A designated ground marker numbered one to six was used to ensure easy identification of the GCPs on the photos.

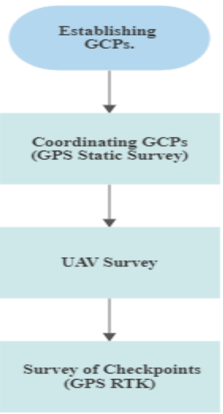

Fig. 2 Work flowchart

2.3.2 Statistical Accuracy Assessment

The variations between the reference value and the UAV photogrammetry solution value at particular GCPs are used to determine the accuracy of the evaluations. Prior to the image-capturing process, the reference values were measured using RTK GNSS receivers, and the RMSE was derived from the discrepancies. The differences between the reference data and the data obtained from UAVs are usually measured using the RMSE. The RMSE was computed using the following equations: (1) to (4).

$$RMSE_x = \sqrt{\frac{\Sigma(X_{UAV} - X_{GPS})^2}{n}} \quad (1)$$

$$RMSE_y = \sqrt{\frac{\Sigma(Y_{UAV} - Y_{GPS})^2}{n}} \quad (2)$$

$$RMSE_z = \sqrt{\frac{\Sigma(Z_{UAV} - Z_{GPS})^2}{n}} \quad (3)$$

$$RMSE_r = \sqrt{RMSE_x{}^2 + RMSE_y{}^2} \quad (4)$$

where, n is the number of compared pairs of coordinates. The horizontal RMSE is distributed in two dimensions (X and Y) and is required to calculate the radial or positional error.

2.3.3 Real-Time Kinematic (RTK) GNSS Technique

RTK is an attractive method of surveying with GNSS receivers as it combines high accuracy with short observation periods (Santos, 2000). RTK GNSS provides real-time corrections, providing up to centimeter-level or millimeter-level accuracy depending on the GNSS receiver used. Many applications use RTK GNSS technology (Morales *et al.*, 2007). When using the GNSS-RTK approach, the system simultaneously receives satellite signals from at least two GNSS receivers. One of them is situated at a known coordinate reference station, and the other one (or ones) attempt to measure an unknown point coordinateWhen operating in RTK mode, the reference station receives the satellite GNSS signal and uses a data link in the field to transmit its observations and coordinate data to the observation locations (Hongtao Xu, 2012). The RTK technique was used in collecting five sample positions.

2.3.4 UAV Surveys

The UAV carries a digital camera into the air and facilitates photographing the project area from above. The DJI Phantom 4 pro-multi-rotor drone is similar to helicopters and has four propellers that push air beneath the aircraft to attain flight. Because the multi-rotor drones fly slowly and close to the ground, they are best suited for very low-altitude missions where minute photographic details are the priority.

Once on the field, the drone is assembled, the missions are loaded into the drone's autopilot system, and the drone is then "taken" off from the ground in a hover. Once the aircraft is in the air, the autopilot assumes control, starts flying the mission, and starts capturing pictures at predetermined intervals. The airplane is observed visually and electronically throughout this operation. In the event that it becomes necessary to override the autopilot, the drone can be called home or piloted manually. When a mission is completed, the drone lands itself. It is retrieved, and the photographs are downloaded from the camera. Once fresh batteries and additional memory cards are replaced, the drone is ready for another mission. The onboard inertial measurement unit, GNSS, and autopilot enable the drone to travel autonomously along a preprogrammed route using the Pix4Capture software. The battery life provides a flight time of 20 minutes. This digital plan is saved like a flight plan. The survey took place on January 10, 2019, during the dry season and the ban on small-scale mining activities. This period of the year was chosen to ensure no interference in the data collection by mining activities (Ronchetti *et al.*, 2018). A single grid flight mission, as shown in Fig.

3, was planned with side and front overlap equal to 75% and 80%, respectively. An average ground sample of roughly 1.64 cm/px was ensured by fixing the flight height at 60 m above the ground. At the conclusion of the survey, 1121 photos totaling 48.74 ha had been collected.

To avoid the sun peaking and producing sun glints, hot spot views, or harsh shadows, it was important to take aerial images in the middle of the day or the middle of the afternoon. Otherwise, the photogrammetric software would have a difficult time computing points in the affected area. This will then produce extra noise and dispersed points around the area, yielding inaccurate data.

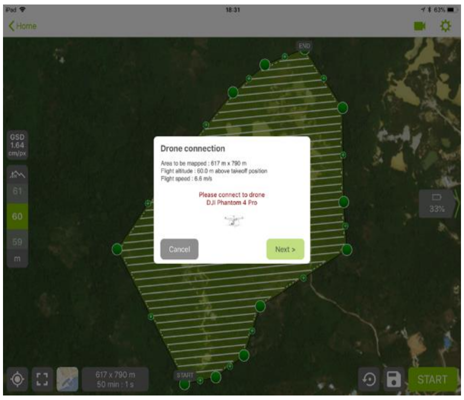

Fig. 3 Planned Flight Mission

The survey was carried out between 14:00 and 16:00 Greenwich Meridian Time and involved four flights to cover the entire research region. During each flight, the drone independently navigated between waypoints created in the flight planning software and uploaded to the onboard flight controller (Bash et al., 2018).During the flight operation, the camera was triggered every 2.5 s as the drone traveled at a speed of 6.6 m/s, and all images were stored in raw format to aid later processing (Bash *et al*., 2018), as shown in Fig. 4.

Fig. 4 Extents of ConFig.d Area

2.3.5 Image Processing

The imagery collected during each survey was processed to produce a final orthophoto and 3-dimensional surface of the study area. The preliminary steps involved are shown in Fig. 5.

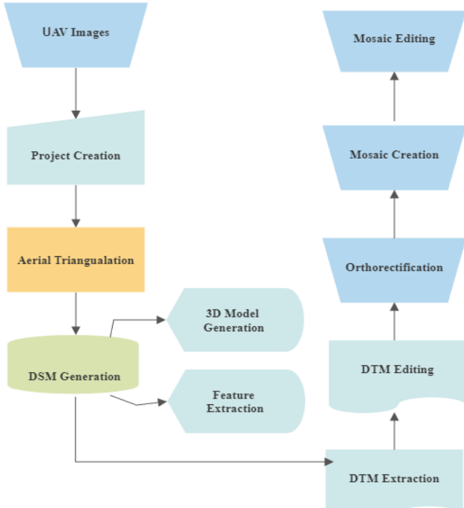

Fig. 5 Flowchart of Correlator 3D Workflow

The first stage in processing the images was by creating a project file. The main aim of creating a project file is to centralize basic information for easy usage. The various steps for creating a project for UAV images are as follows:

- Image Selection: The various kinds of images to be processed were selected and a specified system of projection was set.

- Camera Parameters: These parameters are mostly determined by the software. These parameters include the value for the focal length, principal point, pixel size, and distortion.

Ground Control Points (GCPs) as shown in Fig. 6. Creation: The significance of this process is to avert global spatial offset and is also used as a means of validating the residual error of the refined values.

Fig. 6 The GCP process

After completing the Aerial Triangulation (AT) process, a Digital Surface Model (DSM) was generated at the output resolution. In this process, the overlapping of regions between successive images was carried out and used as stereo data to obtain altitude information. After creating a DSM surface, the next step is to extract the Digital Terrain Model (DTM) by automatically filtering the DSM.

In this process, structures and trees on the land were eliminated from the DSM. One of the significances of DTM is that they are used for generating orthophotos since they avoid visual artifacts caused by using DSM. To formulate an orthomosaic of an area, orthophotos of the individual images must be created by the orthorectification process. This process consists of the geometric correction of the raw images. This helps provide an accurate and precise replica of the ground surface. Moreover, the photos are adjusted for 3-dimensional relief, lens distortions, and camera orientation.

After correcting the raw images, the individual orthophotos were merged to attain a single, unique image of the entire project area. To provide a smooth and seamless transition between adjacent images constituting the mosaic, seamline generation and colour balancing were performed.

2.3.6 Digital Surface Model

Earth's surface is represented digitally in digital elevation models (DEMs). In many geographic Information Systems (GIS), the DEM is one of the most significant spatial datasets. It is referred to as an ordered or unordered digital set of ground elevation for landscape representation (Zhou, 2017).

2.3.7 Digital Terrain Model

A more general term used to describe a DEM with one or more types of terrain information, such as soil characteristics, drainage patterns, and terrain morphological features, is "DTM." This is a DEM when it just deals with one kind of topography data (height). DTMs are broken down into DEMs (Li et al., 2005).The DTM was extracted from the DSM. This avoided visual artifacts (e.g., along building edges, trees) caused by using DSM. The DSM analyses and automatically removes structures lying on the ground to get to the natural surface, as in Fig. 7. A polygonal selection can be made with the DEM editing tool, and operations like cropping or deleting, setting or offsetting elevation values, and filtering regions are all possible. There is also a "Delete and Fill" option for swiftly removing buildings.

2.3.8 Orthorectification

Individual orthophotos were made prior to the creation of the orthomosaic An accurate representation of the ground surface is achieved through orthorectification, which involves geometrically correcting the raw images. In order to correct for topographic relief, lens distortion, and camera orientation, the images are modified. They can be visualized once all orthophotos have been created.

2.3.9 Some Key Formulae and Techniques

The equation for perspective projection: This equation explains how a 3D point in space is projected onto a 2D image plane and is used to translate 3D point coordinates in a scene to 2D pixel coordinates in an image. The equation is:

$$\mathrm{x} = \mathrm{f} * {}^{\mathrm{X}}\!/_{\mathrm{Z}} + \mathrm{x}_0$$

$$\mathrm{y} = \mathrm{f} * {}^{\mathrm{Y}}\!/_{\mathrm{Z}} + \mathrm{y}_0$$

Where

x,y = pixel coordinates in the image X, Y, Z = 3D coordinates of the point in space f = focal length of the camera x_0, y_0 = coordinates of the principal point (the intersection of the optical axis with the image plane).

The collinearity equations: These describe the relationship between the 3D coordinates of a point in space, the pixel coordinates of the corresponding point in the image, and the camera parameters. The collinearity equations are used in bundle adjustment to refine the camera parameters and the 3D coordinates of the points. The basic collinearity equations are

$$X = (x - x_0) * Z/f$$

$$Y = (y - y_0) * Z/f$$

Where

x,y = pixel coordinates in the image X, Y, Z = 3D coordinates of the point in space f = focal length of the camera x_0, y_0 = coordinates of the principal point.

Bundle adjustment is a method used in photogrammetry that reduces the discrepancy between the observed picture features and the expected features based on the estimated 3D positions. It also refines the position and orientation of the cameras in the scene as well as the 3D position of the points. This issue is resolved using the formulae for the bundle adjustments. These are the standard bundle adjustment equations:

$$min \sum ||x - f(X,P)||^2 \quad (5)$$

where:

x is a vector that represents all of the detected image features, such as pixel coordinates.
X is the vector of unknown 3D point locations in a common reference frame.

P is the vector of unknown camera parameters, which include each camera's placement and orientation in the scene as well as internal details like its main point and focus length.

f is the function that maps the 3D points and camera settings into the expected image attributes.

∑ represents the total amount of observed image features across all images.

Triangulation is a method for establishing the three-dimensional (3D) position of a point in space by intersecting the sight rays from two or more photographs where the point appears. To resolve this issue, triangulation equations are employed.
The general triangulation equations are:

$$P_1 * X = x_1 * Z$$

$$P_1 * Y = y_1 * Z$$

$$P_2 * X = x_2 * Z$$

$$P_2 * Y = y_2 * Z$$

Where,

P_1 and P_2 are 3 x 4 projection matrices that describe the relationship between the 3D point (X, Y, Z) and its image coordinates (x_1, y_1) and (x_2, y_2) in two different images.

X, Y, and Z are the unknown coordinates of the 3D point in a common reference frame.

x_1, y_1, x_2, and y_2 are the known image coordinates of the point in the two images.

Z is the unknown depth of the point along the sight rays from the two images

The intrinsic and extrinsic camera parameters, which describe the position and orientation of the camera in the scene and its internal characteristics, such as the focal length and the principal point, are used to derive the projection matrices, which are then used to solve the triangulation equations for the 3D point coordinates (X, Y, and Z) using numerical techniques like least squares or direct linear transformation (DLT).

Verification of data accuracy

RMSE analysis is performed to compare the outputs of the UAV survey to the ground truth measurements taken at the GCPs.

$$RMSE = \sqrt{[(\sum(X_i - Y_i)^2)/n]} \qquad (6)$$

X_i is the UAV survey measurement at a GCP

Y_i is the ground truth measurement at the same GCP, and

n is the number of GCPs.

3 Results and Discussion

Results obtained from the study and the discussion of the results are presented in this section.

3.1 Results

The results are presented in the following sub-sections:

3.1.1 Geo-referencing

Based on the project summary provided, the mapping indicated aerial data utilising a DJI Phantom 4 Pro V2 and a DJI FC6310 camera. GCPs were used in the project for precise georeferencing and spatial alignment of the aerial images.

Tables 1–3 show the project summary obtained from processing the imagery with the GCPs.

Table 1 Project summary

PROJECT SUMMARY				
PROJECT			**GROUND CONTROL POINTS**	
Project type	Aerial		Average XY error	0.008 m
Projection	EPSG: 32630 WGS 84 UTM zone 30N		RMS Z error	0.047 m
Planar units	METERS		Average projection erro	0.51 pixels
Elevation units	METERS		Standard deviation	0.27 pixels
Camera 1	1103 Images (DJI FC6310)		Number of GCPs	6
Total Images	1103			
IMAGE TIE POINTS				
Quality assessment	Excellent			
Average projection error	0.47 pixels			
Standard deviation	0.48 pixels			
Average number of points per images	78			

Table 2 The Error details for the GCPs

DETAILED ERROR						
Point ID	**Type**	**X (m)**	**Y (m)**	**Z (m)**	**XYZ**	**Pixels**
FFH1	GCP	0.050	-0.080	-0.030	0.021	0.543
FFH2	GCP	0.020	0.005	0.020	0.107	0.032
FFH3	GCP	0.020	0.020	-0.010	0.010	0.665
FFH4	GCP	-0.040	-0.050	-0.020	0.027	0.302
FFH5	GCP	-0.030	0.060	0.030	0.018	0.694
FFH6	GCP	0.020	0.020	-0.030	0.022	0.841

Table 3 Control analysis

CONTROL POINT ANALYSIS		
PROJECTION ERROR	GCP	Check Points
Average (pixels)	0.51	0
Standard deviation (pixels)	0.27	0
Min, Max (pixels)	[0.03, 1.28]	[0.00, 0.00]
SPATIAL ERROR		
	GCP	Check Points
RMS X error (m)	0.006	0
RMS Y error (m)	0.007	0
RMS Z error (m)	0.047	0
Average XY error (m)	0.008	0
Average XYZ error (m)	0.034	0

Table 4 Samples for the Check Survey

Sample Points	Samples Position on Image/m	Samples RTK Survey Checked Points/m	Error/m
1	X : 597734.020	X : 597734.035	X : -0.015
	Y: 640065.030	Y: 640065.050	Y: -0.020
	Z: 61.125	Z: 61.153	Z: -0.027
2	X: 598514.028	X: 598514.065	X: -0.037
	Y: 639665.026	Y: 639665.035	Y: -0.009
	Z: 60.236	Z: 60.274	Z: -0.038
3	X: 598524.028	X: 598524.043	X: -0.015
	Y: 639485.024	Y: 639485.041	Y: -0.017
	Z: 59.452	Z: 59.475	Z: -0.023
4	X: 598704.030	X: 598704.046	X: -0.016
	Y: 639485.024	Y: 639485.034	Y: -0.010
	Z: 61.024	Z: 61.056	Z: -0.032
5	X: 599234.035	X: 599234.061	X:-0.026
	Y: 639485.024	Y: 639485.033	Y: -0.009
	Z: 60.356	Z: 60.375	Z: -0.019

The error levels for the georeferencing and the checkpoints were good.

The project shows a good number of tie points per image, outstanding projection accuracy, and high-quality data gathering. A low average XY error was achieved thanks to the precise georeferencing provided by the GCPs. The summary offers useful details on the project's precision and quality, guaranteeing accurate mapping results for additional analysis and interpretation.

3.1.2 Image Processing

Data Analysis and Mapping Outputs: After the georeferencing of the imagery, data analysis was performed to provide the mapping outputs. A few examples of such visualisations are orthomosaic maps, digital surface models (DSMs), point clouds, contour lines, and others. These outputs offer detailed information about the small-scale mining site, including the topography, buildings, and potential dangers.

The DSM or orthorectification generated included the trees and structures as in Fig. 7.

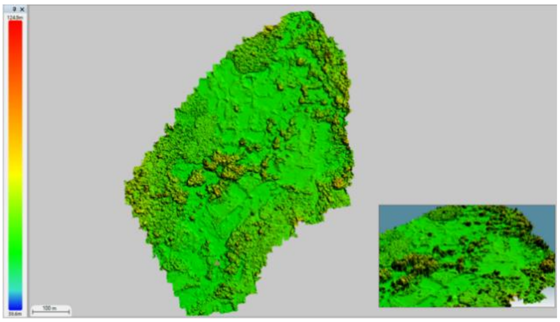

Fig. 7 DSM Generated

3.1.3 Digital Terrain Model

The DTM was extracted from the DSM as shown in Fig. 8.

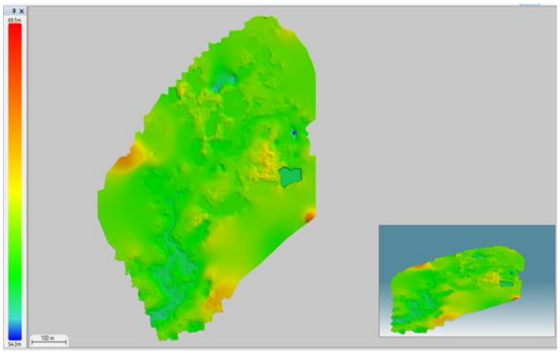

Fig. 8. DTM surface extracted from DSM

3.2 Discussion

The orthomosaic generated shows the visualization of the area, it provides an accurate representation of the ground surface. This reveals the devastating environmental impact of small-scale mining (galamsey) in the study area, as shown in Fig. 9. The entire waterbodies were destroyed and heavily polluted. The area is also dotted with abundant uncovered dug-out pits which pose a danger to the comminutes. The orthomosaic also shows tracks of farmland destroyed by illegal miners. It is evident that UAV can be used effectively to collect data from inaccessible areas such as the mine-out areas and the can be analysed and interpreted for the purposes of environmental restoration.

Fig. 9 Orthorectification of the Images

4 Conclusions

In conclusion, mapping inaccessible abandoned small-scale mining sites can be accomplished using remote sensing technologies such as; photogrammetry, UAV surveys, and GNSS techniques. Traditional surveying techniques have difficulties with site accessibility, data accuracy, and survey team security. UAVs are especially helpful for locations with challenging terrain since they enable precise 3D modelling without actual site access. Using UAVs and photogrammetry sensors together offers a quicker and safer way to gather accurate survey data. This method provides accurate data, lowers survey team hazards, and offers cost-effective alternatives to traditional surveying procedures. The study carried out shows how integrated GNSS receivers and UAVs can be used for mapping small-scale mining sites and, hence, assisting in the reclamation of geomorphologic landforms.

References

Amiri, G. G., Saharkhiz, M. J. and Pourghasemi, H. R. (2019). "A Comparative Study of Cost-Effective Techniques for Estimating the Volume of Open-Pit Mines: Terrestrial Laser Scanning vs. Unmanned Aerial Vehicles Photogrammetry. Resources Policy", Vol. 61, pp. 430-443.

Bash, E. A., Moorman, B. J. and Gunther, A. (2018), "Detecting Short-term Surface Melt on an Arctic Glacier Using UAV Surveys", *Remote Sensing*, Vol. 10, No. 1547, pp. 2-17.

Beyer, K., Lathan, L. and Doherty, M. (2017), "Mapping inaccessible mining areas using unmanned aerial vehicles and 3D photogrammetry", Journal *of Unmanned Vehicle Systems*, Vol. 5, No. 4, pp. 158-167.

Culig, J., Briš, R. and Čerba, O. (2018), "Possibilities of Using UAVs for Surveying in Open-Pit Mines", *Acta Montanistica Slovaca*, Vol. 23, No.2, pp. 128-136.

Díaz-Vilariño, L., Martínez-Sánchez, J. and Montes-Bernárdez, R. (2019), "Application of Drones in the Safety Inspection of Abandoned Underground Mines", *Minerals*, Vol. 9, No.11, 694pp.

Elfadaly, A. and Elbeltagi, E. (2017), "Accuracy and Cost Comparison of Photogrammetry versus Laser Scanning for 3D Modelling", *Measurement*, Vol.109, pp. 239-251.

Ghosh, S. K., Mondal, A. and Debnath, P. (2018), "Comparative Study of UAV Mapping and Terrestrial Surveying for Volume Estimation of an Open-Cast Coal Mine", *Geocarto International*, Vol. 33, No. 2, pp. 149-164.

Hancock G. R, Duque, J. M. and Willgoosed, G. R. (2019), "Geomorphic design and modeling at catchment scale for best mine rehabilitation – The Drayton mine New South Wales, Australia" *Environmental Modelling & Software*, pp140-151.

Hao, M., Wang, C. and Li, C. (2019). "A Comparative Analysis of UAV-Based Photogrammetry and LiDAR for Measuring Cut and Fill Volumes in Surface Mining", *Remote Sensing*, Vol. 11, No.11, 1341pp.

Hongtao Xu, (2012), "Application of GPS-RTK Technology in the Land Change", *Procedia Engineering*, Vol. 29, pp. 3454-3459.

Hu, Y., Zhou, C., Wu, Y., Li, M. and Wang, J. (2020), "Application of Photogrammetry Based on Unmanned Aerial Vehicle in Open-Pit Mining". *IEEE Access*, Vol. 8, pp. 77951-77959.

Khodabandeloo, M., Rastiveis, H. and Ataei, M. (2019), "Investigation of Unmanned Aerial Vehicles (UAVs) for Mine Site Mapping and Monitoring" *International Journal of Mining Science and Technology*, Vol. 29, No. 5, pp. 773-783.

Koltunov, Y., Dmitry, N., Aleksey, D. and Dmitry, M. (2019). "Digital photogrammetry and terrestrial laser scanning for mapping of aban-doned mine workings", *Geosciences*, Vol. 9, No. 4, 183pp.

Korpela, I. (2004). "Individual tree measurements by means of digital aerial photogrammetry" *Silva Fennica*, Vol. 3, pp. 1-96.

Madawalagama, S., Munasinghe, N., Dampegama, S. D. P. J. and Samarakoon, L. (2016), "Low-cost Aerial Mapping with consumer grade drones", 37*th* *Asian Conference on Remote Sensing*, pp. 1-8.

Morales, Y. T. and Tsubouchi, T. (2007), "DGPS, RTK-GPS and Star Fire DGPS Performance Under Tree Shading Environments", *Proceed-*

ings of the 2007 IEEE International Conference on Integration Technology*, pp. 519-524.

Li, Z., Zhu, Q. and Gold, C. (2005), "Digital Terrain Modeling: Principles and Methodology", CRC Press, Boca Raton, 1st edition, 323pp.

Ronchetti, G., Pagliari, D., and Sona, G. (2018), "DTM Generation Through UAV Survey with a Fisheye Camera on a Vineyard", *The International Archives of the Photogrammetry, Remote Sensing and Spatial Information Sciences*, Riva Del Garda, Italy, pp. 983-989.

Santos, M. C. (2000), "A Practical Evaluation of the GPS Rapid Static Method", *GEOMATICA*, Vol. 54, No. 4, pp. 427-431.

Singh, A., Singh, T. and Singh, R. (2020), "Cost-Effective and Rapid Surface Area Estimation of Mining Pits Using a Combination of Ground Control Points (GCPs) and UAV Photogrammetry", *Journal of the Indian Society of Remote Sensing*, Vol. 48, No.7, pp.1265-1273.

Zhou, Q. (2017), "Digital Elevation Model and Digital Surface Model", *The International Encyclopedia of Geography*, pp. 1-17.

Authors

Francis Ferguson Howard is a PhD candidate at the University of Mines and Technology, Tarkwa. He holds MSc in Mining Engineering from KNUST, Kumasi and MPhil in Geomatic Engineering from UMaT, Tarkwa. He is the Managing Director of Samaward Ghana Limited. He is a Member of Ghana Institution of Surveyors. His research interest is in Application of UAV in mapping, identification of fluvial Erosion using Artificial Intelligence and Geospatial techniques.

Cynthia Borkai Boye is an Associate Professor of Geomatic Engineering and a Licensed Surveyor currently working at the University of Mines and Technology, Tarkwa, Ghana. She holds BSc in Geodetic Engineering from KNUST, Professional Masters in GeoInformatics from ITC Netherlands and a PhD in Oceanography from the University of Ghana, Legon. She is a member of Ghana Institution of Surveyors, Ghana Institution of Engineering, a member of the Association of Licensed Surveyors. Her research and consultancy work include Shoreline Change Analyses and Prediction, GIS Applications, Fluvial Sediment Analyses and Prediction, Cadastral and Engineering Surveying, and Dispute Surveys.

Yakubu Issaka is an Associate Professor of Geomatic Engineering and a Consulting Engineer currently working at University of Mines and Technology, Tarkwa-Ghana. He holds BSc degree in Geomatic Engineering from KNUST, Kumasi-Ghana, MPhil and PhD in Geomatic Engineering from UMaT, Tarkwa-Ghana. He holds an MSc in Land Policy and Administration from the University of Cape Coast. He also has a Certificate in Disaster Risk Management and Environmental Assessment for Spatial Planning from the ITC-University of Twente, The Netherlands.

J. S. Y. Kuma is a retired Professor in Environmental Hydrogeology and Geophysics at the University of Mines and Technology (UMaT), Tarkwa. He was awarded a BSc (Hons) in Geology and Physics at the University of Ghana, Legon. He received the Pg Dip and MSc degrees in Geophysics at Delft, The Netherlands. Professor Kuma received a PhD in Water Resources Engineering from the University of Newcastle upon Tyne, England. He is involved in mine water hydrogeological research and water management issues.